Supporting Information

Spectroscopic and Mechanistic Investigations of Dehaloperoxidase B from *Amphitrite ornata*

Jennifer D'Antonio, Edward L. D'Antonio, Matthew K. Thompson, Edmond F. Bowden, Stefan Franzen, Tatyana Smirnova and Reza A. Ghiladi*

[‡]Department of Chemistry, North Carolina State University, Raleigh, North Carolina, 27695-8204

Running Title: Spectroscopic and Mechanistic Investigations of Dehaloperoxidase B
Address Correspondence to: Reza A. Ghiladi Department of Chemistry, North Carolina State University, Raleigh, NC 27695-8204, Tel. 919-513-0680; Fax. 919-515-5079; E-Mail: Reza_Ghiladi@NCSU.edu

Table of Contents

reaction with a 10-fold excess of H_2O_2 (*in situ* generated Compound ES) at pH 7. (B) Calculated UV-visible spectra for ferric DHP B incubated with TCP (black), ferric DHP B regenerated upon product formation (green), and the ferric/oxyferrous DHP B mixture (purple) are shown; the rapid-scanning data from panel A were compiled and fitted to a two-step, three species sequential irreversible model using the Specfit global analysis program.

Figure SD8. DCQ product formation (A, ΔAbs_{275}) and TCP co-substrate loss (B, ΔAbs_{312}) for the reaction between ferric DHP B (10 μM) pre-incubated with TCP (300 μM) followed by their reaction with 100 μm H_2O_2 (*in situ* generated Compound ES) at pH 7 and 25 °C. The pre-incubation period between ferric DHP B and TCP was varied as indicated in the legend.

Figure SD9. (A) Stopped-flow UV-visible spectroscopic monitoring (900 scans, 85 sec) of the double-mixing reaction between ferric DHP B (10 μM) pre-incubated with a 7-fold molar excess of DCQ for 500 ms prior to its reaction with a 2.5-fold excess of H_2O_2 (*in situ* generated Compound ES) at pH 7. (B) UV-visible spectra observed for ferric DHP B incubated with DCQ (black, 2 ms), Compound ES (dark grey, 4 s), and the ferric/oxyferrous DHP B mixture (light grey, 85 s) are shown.

Figure SD10. (A) Stopped-flow UV-visible spectroscopic monitoring (900 scans, 85 sec) of the reaction between ferric DHP B (10 μM) and a 7-fold excess of DCQ at pH 7. (B) Calculated UV-visible spectra for ferric (black) and the ferric/oxyferrous DHP B mixture (purple) are shown; the rapid-scanning data from panel A were compiled and fitted to a one-step, two species irreversible model using the Specfit global analysis program.

Figure SD11. (A) UV-visible spectrum of Compound RH formed from the reaction of ferric DHP B and a 10-fold excess of hydrogen peroxide at pH 7. (B) Reduction of Compound RH upon addition of excess sodium dithionite. (C) After desalting via gel filtration, UV-visible spectrum of Compound P_{426} at pH 7.0.

Figure SD12. (A) UV-visible spectrum of Compound RH formed from the reaction of ferric DHP B and a 2.5-fold excess of hydrogen peroxide at pH 7. (B) Reduction of Compound RH upon addition of excess sodium dithionite. (C) After desalting via gel filtration, UV-visible spectrum of oxyferrous DHP B at pH 7.0.

Figure SD1. UV-visible spectra of different heme states of DHP B (10 μM) at pH 7.0.

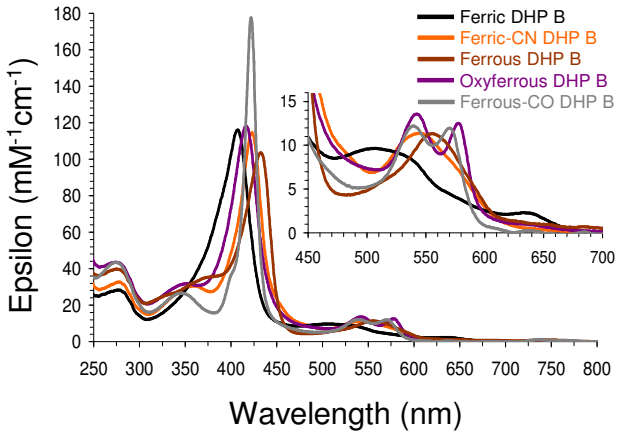

Figure SD2. UV-visible spectra of halophenol adducts of DHP B (8 μM) at pH 7.0. A) Monohalophenol adducts of 4-FP (8 mM), 4-CP (8 mM), 4-BP (8 mM), 4-IP (850 μM) and phenol (8 mM). B) Trihalophenol adducts of TFP (4 mM), TCP (0.3 or 2 mM), and TBP (255 μM).

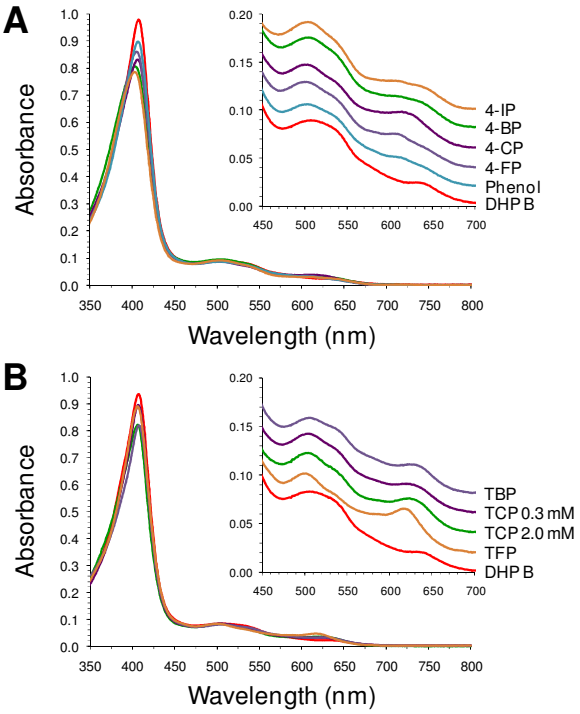

Figure SD3. UV-visible spectroscopic monitoring of the oxidative dehalogenation of trihalophenols (150 μM) as catalyzed by DHP B (0.5 μM) in the presence of hydrogen peroxide at pH 7 and 25 °C. (A) Trifluorophenol, ferric DHP, (B) trichlorophenol, ferric DHP, (C) trichlorophenol, ferrous DHP, and (D) tribromophenol.

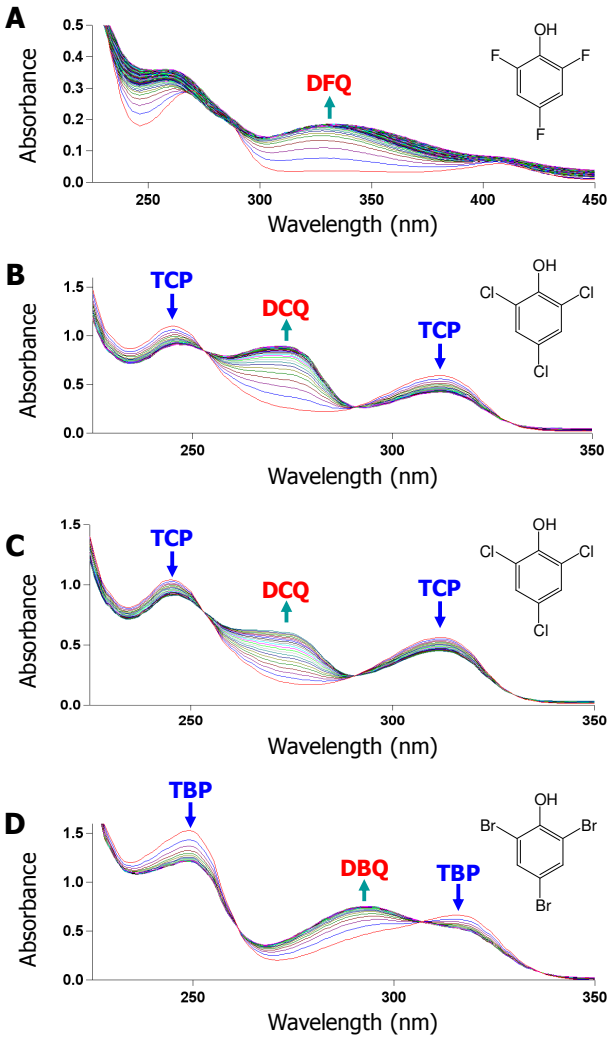

Figure SD4. Dependence of k_{obs} for the reaction between ferric DHP B (10 μM) with hydrogen peroxide (2.5 – 25 equivalents) at pH 7 yielding Compound ES. Note: experiments were performed in triplicate, with error bars smaller than the symbols used in the plot.

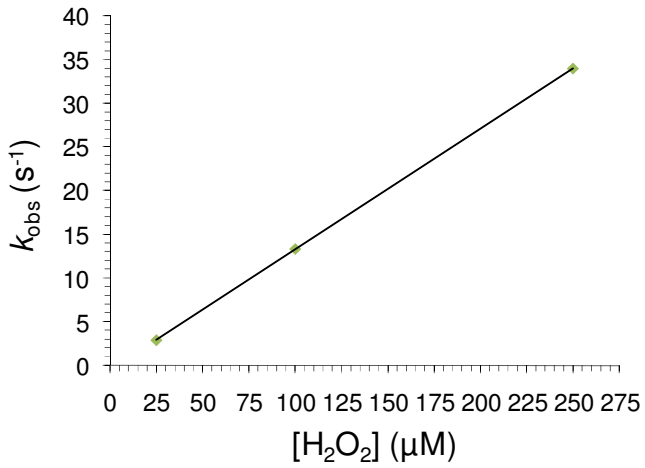

Figure SD5. (A) Stopped-flow UV-visible spectroscopic monitoring (900 scans, 85 sec) of the double-mixing reaction between preformed DHP B Compound ES (10 µM; 500 ms) and TCP (300 µM) at pH 7. See Materials and Methods for details. (B) Calculated UV-visible spectra for Compound ES (red), ferric DHP B regenerated upon product formation (green), and the ferric/oxyferrous DHP B mixture (purple) are shown; the rapid-scanning data from panel A were compiled and fitted to a two-step, three species sequential irreversible model using the Specfit global analysis program.

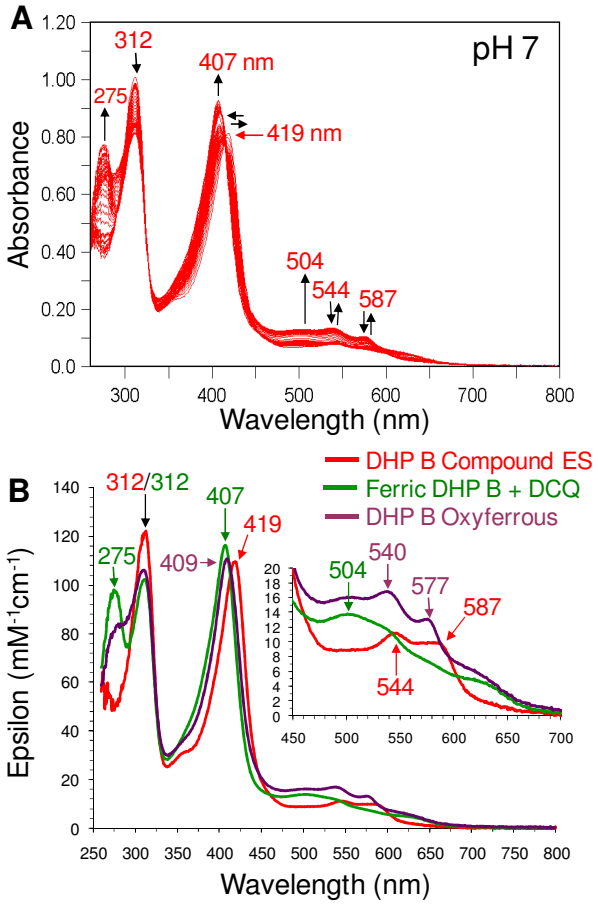

Figure SD6. DCQ product formation (A, ΔAbs_{275}) and TCP co-substrate loss (B, ΔAbs_{312}) for the reaction between preformed Compound ES (10 μM) with TCP (300 μM) at pH 7 and 25 °C. The aging time of the Compound ES intermediate was varied as indicated in the legend.

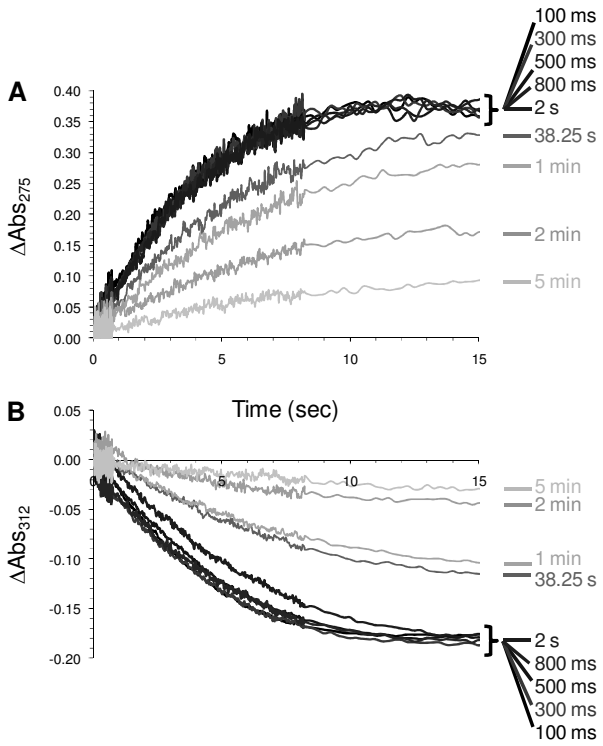

Figure SD7. (A) Stopped-flow UV-visible spectroscopic monitoring (900 scans, 85 sec) of the double-mixing reaction between ferric DHP B (10 µM) pre-incubated with TCP (300 µM) for 500 ms prior to its reaction with a 10-fold excess of H_2O_2 (*in situ* generated Compound ES) at pH 7. (B) Calculated UV-visible spectra for ferric DHP B incubated with TCP (black), ferric DHP B regenerated upon product formation (green), and the ferric/oxyferrous DHP B mixture (purple) are shown; the rapid-scanning data from panel A were compiled and fitted to a two-step, three species sequential irreversible model using the Specfit global analysis program.

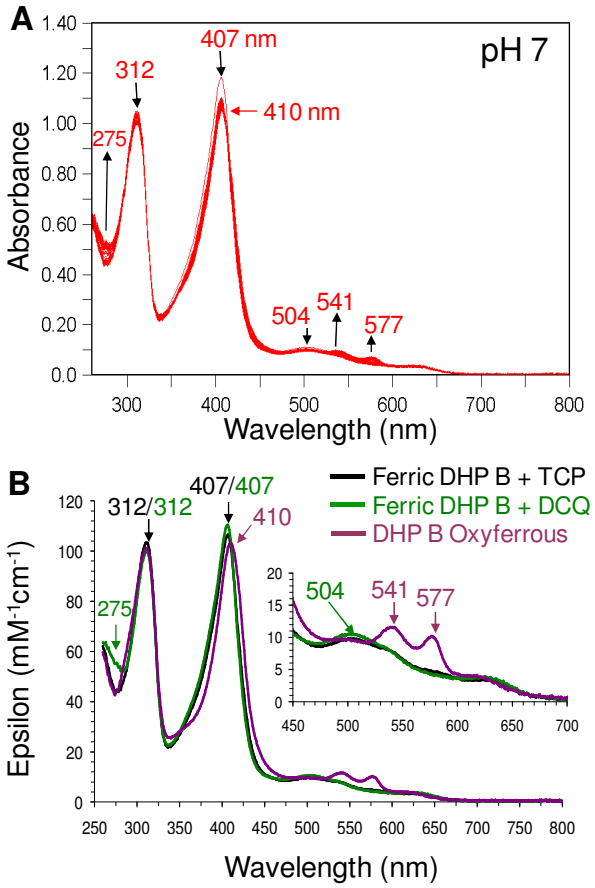

Figure SD8. DCQ product formation (A, ΔAbs_{275}) and TCP co-substrate loss (B, ΔAbs_{312}) for the reaction between ferric DHP B (10 μM) pre-incubated with TCP (300 μM) followed by their reaction with 100 mm H_2O_2 (*in situ* generated Compound ES) at pH 7 and 25 °C. The pre-incubation period between ferric DHP B and TCP was varied as indicated in the legend.

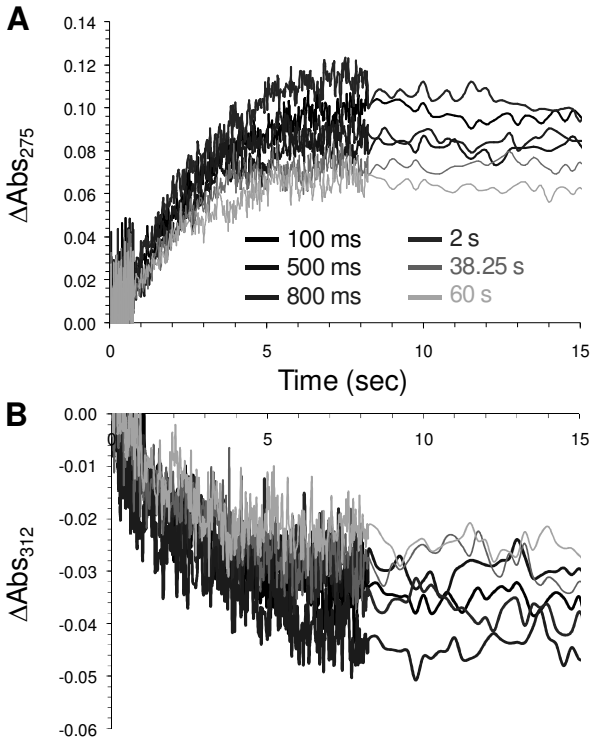

Figure SD9. (A) Stopped-flow UV-visible spectroscopic monitoring (900 scans, 85 sec) of the double-mixing reaction between ferric DHP B (10 μM) pre-incubated with a 7-fold molar excess of DCQ for 500 ms prior to its reaction with a 2.5-fold excess of H_2O_2 (*in situ* generated Compound ES) at pH 7. (B) UV-visible spectra observed for ferric DHP B incubated with DCQ (black, 2 ms), Compound ES (dark grey, 4 s), and the ferric/oxyferrous DHP B mixture (light grey, 85 s) are shown.

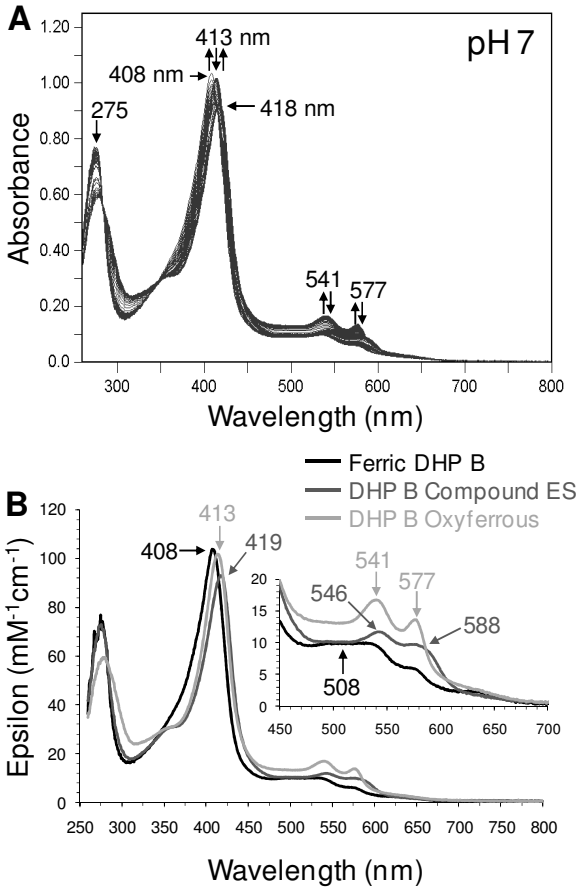

Figure SD10. (A) Stopped-flow UV-visible spectroscopic monitoring (900 scans, 85 sec) of the reaction between ferric DHP B (10 µM) and a 7-fold excess of DCQ at pH 7. (B) Calculated UV-visible spectra for ferric (black) and the ferric/oxyferrous DHP B mixture (purple) are shown; the rapid-scanning data from panel A were compiled and fitted to a one-step, two species irreversible model using the Specfit global analysis program.

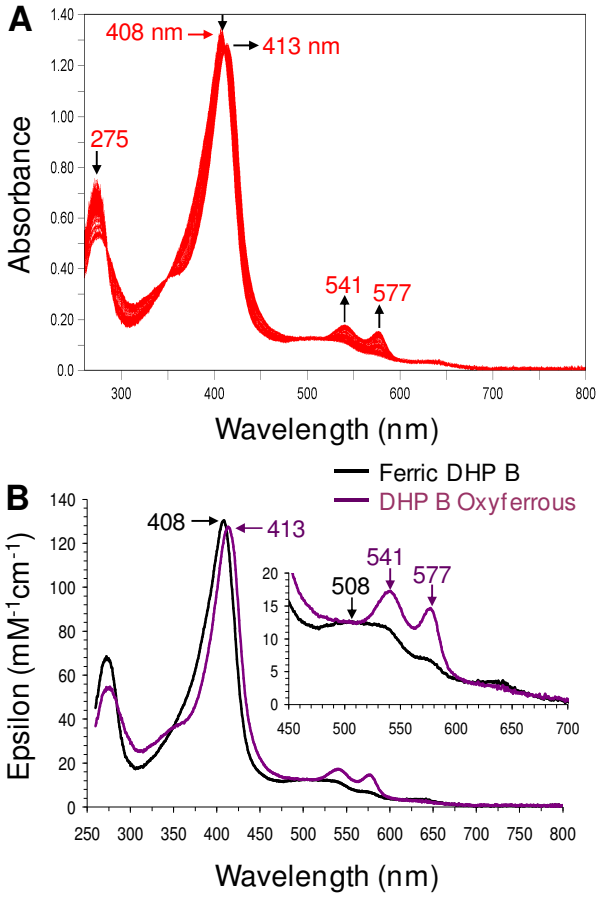

Figure SD11. (A) UV-visible spectrum of Compound RH formed from the reaction of ferric DHP B and a 10-fold excess of hydrogen peroxide at pH 7. (B) Reduction of Compound RH upon addition of excess sodium dithionite. (C) After desalting via gel filtration, UV-visible spectrum of Compound P_{426} at pH 7.0.

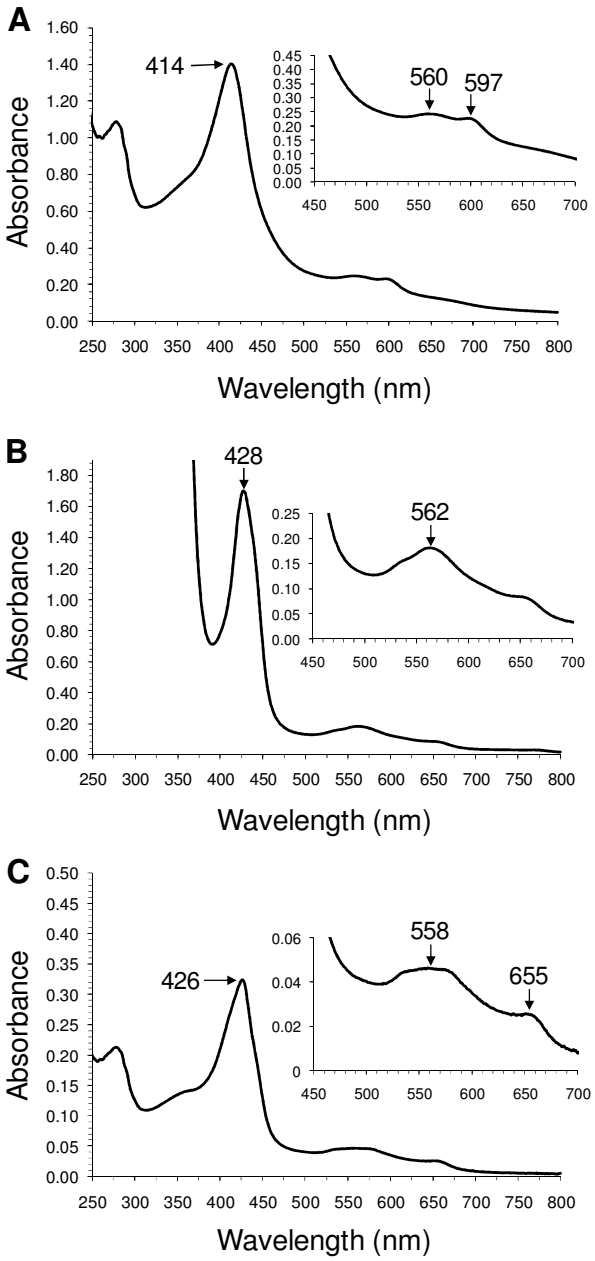

Figure SD12. (A) UV-visible spectrum of Compound RH formed from the reaction of ferric DHP B and a 2.5-fold excess of hydrogen peroxide at pH 7. (B) Reduction of Compound RH upon addition of excess sodium dithionite. (C) After desalting via gel filtration, UV-visible spectrum of oxyferrous DHP B at pH 7.0.